

Date: November 18, 2018

# Is Thermal Emission in Gamma-Ray Bursts Ubiquitous?

Felix Ryde

*Stockholm Observatory, AlbaNova, SE-106 91 Stockholm, Sweden*

## ABSTRACT

The prompt emission of gamma-ray bursts has yet defied any simple explanation, despite the presence of a rich observational material and great theoretical efforts. Here we show that all the types of spectral evolution and spectral shapes that have been observed can indeed be described with one and the same model, namely a hybrid model of a thermal and a non-thermal component. We further show that the thermal component is the key emission process determining the spectral evolution. Even though bursts appear to have a variety of, sometimes complex, spectral evolutions, the behaviors of the two separate components are remarkably similar for all bursts, with the temperature describing a broken power-law in time. The non-thermal component is consistent with emission from a population of fast cooling electrons emitting optically-thin synchrotron emission or non-thermal Compton radiation. This indicates that these behaviors are the fundamental and characteristic ones for gamma-ray bursts.

*Subject headings:* gamma rays: bursts – gamma rays: observations

## 1. Introduction

It was early recognized that the spectra of gamma-ray bursts (GRBs) have a non-thermal character, with emission over a broad energy range (e.g. Fishman & Meegan (1995)). This typically indicates emission from an optically-thin source and an initial proposal for GRBs was therefore an optically-thin synchrotron model from shock-accelerated, relativistic electrons (e.g. Katz (1994); Tavani (1996)). The number density of the radiating electrons is assumed to be typically a power law as a function of the electron Lorentz factor  $\gamma_e$  above a minimum value,  $\gamma_{\min}$ , with index  $-p$ . Such a distribution gives rise to a power-law photon spectrum with index  $\alpha = -2/3$  below a break energy  $E_p \propto \gamma_{\min}^2$  and a high-energy power-law with index  $\beta = -(p + 1)/2$ . However, this model has difficulties in explaining the observed

spectra of GRBs which show a great variation in  $\alpha$  and  $\beta$  (Preece et al. 2000). In particular, a substantial fraction of them have  $\alpha > -2/3$ , which is not possible in the model in its simplest form, since  $\alpha = -2/3$  is the power-law slope of the fundamental synchrotron function for electrons with an isotropic distribution of pitch angles (Pacholczyk 1970). The problem becomes even more severe for the case when the cooling time of the electrons is shorter than the typical dynamic timescale. In the typical setting of GRBs having a relativistic outflow with a bulk Lorentz factor  $\Gamma \sim 100$ , the time scales for synchrotron and inverse Compton losses are  $\sim 10^{-6}$  s (Ghisellini et al. 2000b), which is much shorter than both the dynamic time scale  $R/2\Gamma^2 c \sim 1$  s ( $R/10^{15}$  cm), and the integration time scale of the recorded data, typically 64 ms to 1 s. In such a case the low-energy power law should be even softer, with  $\alpha = -1.5$  (Bussard 1984; Ghisellini et al. 2000a), now contradicting a majority of the observed spectra. The spectra are also observed to evolve dramatically during the course of a burst, both in  $E_p$ , as well as in the power-law indices, in particular  $\alpha$ . In approximately 60% of all bursts,  $\alpha$  varies significantly, mainly by becoming softer (e.g. Crider et al. (1997)). Some bursts are found to have quasi-thermal spectra during the initial phases, before they become non-thermal (Ghirlanda et al. 2003; Kaneko et al. 2003; Ryde 2004).

The peak energy from the above distribution of electrons is given by  $E_p = \gamma_m^2 B_\perp \Gamma$ . In the external shock model  $\gamma_m$  and  $B_\perp$  are proportional to the bulk Lorentz factor, which makes  $E_p \propto \Gamma^4$ , which poses a problem in explaining the relative narrowness of the observed distribution of peak energies (Preece et al. 2000), even including the X-ray flashes. Similarly, for the internal shock model  $\gamma_m \propto \Gamma_{\text{rel}}$ , the relative Lorentz factor between the two shells that collide, and  $E_p \propto B_\perp \Gamma$ , expected to give a larger scatter as well.

A third complication arises in explaining the observed correlation between the burst's peak-energy and luminosity, also known as the Amati relation (e.g. Lloyd-Ronning et al. (2000); Amati et al. (2002); Ghirlanda et al. (2004)); the peak energy is correlated with the isotropically equivalent energy  $E_p \propto E_{\text{iso}}^{0.40 \pm 0.05}$ . For the synchrotron, internal-shock model one expects  $E_p \propto \Gamma^{-2} L^{1/2} t_v^{-1}$  (e.g. Zhang & Mészáros (2002)), where  $t_v$  is the typical variability time scale. This requires that both  $\Gamma$  and  $t_v$  have to be quite similar for all bursts, which is difficult to imagine. In addition, assuming a typical  $L \propto \Gamma^2$  (e.g. Kobayashi et al. (2002)) would even lead to an anti-correlation (see also Ramirez-Ruiz & Lloyd-Ronning (2002)). Additional assumptions are needed to explain the positive correlation.

Other variations of the synchrotron or/and inverse Compton model have been suggested (see e.g. Baring & Braby (2004); Lloyd-Ronning & Petrosian (2000); Stern & Poutanen (2004)), however, none have been able to describe all aspects of the observations in a convincing manner. To account for these aspects, I argue that GRBs, in general, have a strong thermal component, which is accompanied by a non-thermal component of similar strength.

## 2. Spectral Modelling

Recently, in Ryde (2004) I identified bursts which are dominated by quasi-thermal emission throughout their duration. The temperature of the emitting matter exhibits a similar behavior for all of them, with an initially constant, or weakly decreasing, temperature ( $\sim 100$  keV, power-law index  $\sim 0$  to  $-0.3$ ) and a distinct break into a faster power-law decay with an index of approximately  $-0.6$  to  $-1$ . I also suggested that bursts that are observed to be initially thermal, are similar to these but have an additional non-thermal component that varies in spectral slope and grows in relative strength with time. This category of bursts is illustrated in this paper by GRB980306 (all bursts discussed here were recorded by the BATSE detector on the *Compton Gamma-ray Observatory*). Spectra from three different times are shown in the lower-most panels in Figure 1. The model shown consists of a power law  $\propto E^s$ , representing the non-thermal emission, combined with a Planck function  $\propto (kT)^2 x^2 / (\exp(x) - 1)$ , where  $x = E/kT$ ,  $k$  is Boltzmann’s constant and  $T$  is the temperature. It is clear that the relative strength of the non-thermal component increases with time and that the index  $s$  varies, in this particular burst from  $\sim -1.5$  to  $\sim -3$  (see Figure 2). This leads to the apparent softening below the peak energy. Figure 2 also shows that the temperature of the black body, for this burst, exhibits a similar evolution like the purely quasi-thermal bursts discussed by Ryde (2004), with a distinct break in the cooling curve. There is a total of 10 bursts that have been discussed in the literature from this category (Ghirlanda et al. 2003; Ryde 2004).

We will now study the spectra of more typical bursts, bursts which do not have any exceptionally hard  $\alpha$ -values, nor have any conspicuous spectral evolution, and therefore a thermal component is not required in a first appraisal. For this purpose we analyze the sample of the 25 strongest pulses in the catalogue of Kocevski, Ryde, & Liang (2003), which comprise a complete sample of pulses with a varying spectral shapes and evolution. We compare the results of the fits of the hybrid model to those of the most commonly used Band et al. (1993) model, which is an empirical function consisting of a low-energy power-law with index  $\alpha$ , exponentially connected to a high-energy power-law with index  $\beta$  at an energy  $E_p$ . We note that these two models have the same number of parameters;  $kT$ ,  $s$ , and two amplitudes, compared to  $\alpha$ ,  $\beta$ ,  $E_p$ , and one amplitude. The reduced  $\chi^2$  values and the residuals of the fits indicate equally good fits for both models; the  $\chi^2$ -values are in most cases indistinguishable statistically. The hybrid model was formally better (had a lower  $\chi^2_\nu$  value) in 10 of the cases. The largest differences were for GRB950211 ( $\chi^2_{\text{hyb}}; \chi^2_{\text{band}} = (1.03; 1.10)$ ) for 540 degrees of freedom (d.o.f.) and GRB960530 ( $\chi^2_{\text{hyb}}; \chi^2_{\text{band}} = (0.975; 0.999)$ ) for 2071 d.o.f. and finally for GRB950818 ( $\chi^2_{\text{hyb}}; \chi^2_{\text{band}} = (1.09; 0.96)$ ) for 1819 d.o.f. If a hybrid model with a sharply broken power law with say  $\alpha \equiv -1.5$  and  $\beta \equiv -2.1$  (motivated in §3) is used instead, the  $\chi^2_\nu$  of the latter fit becomes lower: 1.02. This illustrates the obvious fact that

the simple power-law model is an approximation of the actual non-thermal emission if the break energy is within the studied window for a significant fraction of the burst duration. In comparing the two models it should also be noted that the hybrid model is a physical model rather than an empirical model and that the fit results are reasonable from a theoretical point-of-view (see §3). Figure 2 shows three of the studied bursts; GRB921207, GRB950624, which illustrate the most common behavior in which  $s$  evolves from  $-1.5$  to  $\sim -2.1$ , and GRB960530 for which  $s$  is consistent of being constant  $\sim -1.5$  even though a weak hardening is indicated. For all the cases the temperature again has a distinct break in its evolution. Three spectra from GRB950624 are also shown in Figure 1, illustrating the non-thermal character of the summed spectrum through out the pulse.

In conclusion, the spectral evolution is very similar from burst to burst and is independent of the relative strength of the thermal component. This is in stark contrast to the variety of apparent spectral behaviors found by using the Band function, for instance, with strong variation in  $\alpha$ . This fact is a strong indication that the thermal emission, combined with a non-thermal component, is ubiquitous and that the behavior of these components are the characteristic signatures of GRBs.

### 3. Discussion and Conclusion

It is argued above that thermal radiation is the key feature during the prompt phase of most GRBs. Apart from the actual fits presented above and the similarity in behaviors among bursts, such an interpretation is attractive for several reasons. First, the value of the low-energy power-law index,  $\alpha$ , that would be found if the Band function were to be used is now only a result of the relative strength of the thermal component and the slope of the non-thermal component. If the thermal component is strong and/or the non-thermal component is hard, the resulting spectrum will have a hard  $\alpha$  and vice versa. This gives a new interpretation of the observed  $\alpha$  distribution which has been a puzzle. Second, the peak of the spectrum is now determined by  $kT$  and is less sensitive to the bulk Lorentz factor, motivating the narrow dispersion of peak energies. In fact, if the photosphere occurs during the acceleration phase it is practically independent of  $\Gamma$ . Third, the Amati correlation has a natural explanation since for a thermal emitter the luminosity and the temperature are correlated. Rees & Mészáros (2005) show that, somewhat depending on the details of the dissipation processes, a positive correlation close to the observed one arises naturally.

A strong photospheric emission at  $\gamma$ -ray wave lengths is predicted in most GRB scenarios, such as in kinetic models (Mészáros, & Rees 2000; Daigne & Mochkovitch 2002), in MHD models (Drenkhahn & Spruit 2002), as well as in Poynting flux models (Lyutikov &

Usov 2000). In the simplest outflow models the observer-frame temperature should be constant (independent of collimation) during the acceleration phase, since the adiabatic losses are compensated by the acceleration. The typical temperature is

$$kT_0 = \frac{k}{1+z} \left( \frac{L_0}{4\pi r_0^2 c a} \right)^{1/4} \sim 100 \text{ keV} \quad (1)$$

for  $L_0 = 10^{51}$  erg,  $r_0 = 10^8$  cm and  $z = 1$ . After saturation (the free energy of the outflow has been transferred to kinetic energy) the temperature will follow a simple adiabatic relation, during which the outflow coasts along with a constant  $\Gamma = L_0/\dot{M}c^2$ , where  $L_0$  and  $\dot{M}$  are the luminosity and mass outflow rates. The observed emission from an optically-thick shell that expands outwards would emit according to this type of a pattern, similarly to the observed temperature drops in Figure 2. The timescale for the saturation, which according to the observed pulses should be around 1 s, leads to the necessity of very under-loaded fireballs ( $\sim 10^{-9} M_\odot$ ). However, the radiative efficiency is, by necessity, very low for such a scenario, due to large optical depths and that most energy is in kinetic form. On the other hand, if the outflow is indeed radiation-dominated then the saturation will naturally occur at the photosphere. This is also the typical case for electromagnetic outflows (Drenkhahn & Spruit 2002). Furthermore, Rees & Mészáros (2005) argued that dissipation processes (magnetic reconnections, shocks) below the photosphere could radically enhance the thermal luminosity and thus the radiative efficiency (see also Pe’er & Waxman (2004)). Comptonization would convert a fraction of the dissipated kinetic energy back into thermal energy and thus re-energize the photosphere, giving typical peak energy of hundreds of keV. But to keep the spectra quasi-thermal during the evolution, as is observed, there must be sufficient photons available to keep the spectra close to those of a black-body. Grimsrud & Wasserman (1998) (see also Mészáros, Laguna, Rees (1993)) noted that the photons may still be coupled to the matter ( $e^\pm$  or baryons), ensuring a quasi-thermal distribution, beyond the radius where the optical depth has become unity. This occurs when the Compton drag time is shorter than the dynamic time. The flow then saturates when the decoupling occurs, now at a very low optical depth. The electron distribution must after this not be perturbed too much from its thermal distribution to be able to reproduce the observed spectra.

The non-thermal component could be interpreted as the synchrotron spectrum from a distribution of fast-cooling electrons. The initial values of  $s \sim -1.5$  are expected from electrons that are cooled to energies below the  $\gamma_{\min}$  of the injected electrons. The change in index to  $\sim -2$  could indicate that the frequency corresponding to  $\gamma_{\min}$  now moves through the observed energy range and that we, at late times, are detecting the high-energy power-law of the cooling spectrum with  $s = -(p+2)/2$ . For instance, for a Fermi type of particle acceleration in relativistic shocks  $p \sim 2.2$  and  $s = -2.1$  (Mészáros 2002).

In Figure 3, we plot the energy-flux light-curves of three of the bursts studied. The relative strengths of the thermal component vary substantially among them, with GRB980306 having a strong thermal, initial phase. The obvious correlation between the thermal and the non-thermal components is noteworthy, indicating that the emissions cannot be completely independent. Rees & Mészáros (2005) suggested that the non-thermal emission, which is superimposed on the thermal Compton-spectrum, is due to synchrotron shock-emission further out from the photosphere. Internal outflow variations, leading to the internal shocks, would be accompanied by corresponding variations in the thermal emission. An alternative scenario is that non-thermal electrons, accelerated at a shock close to the photosphere, are cooled quickly by the thermal radiation, thereby emitting a non-thermal Compton radiation, boosting every photon by a factor of  $\gamma^2$ . The radiation energy-density could then be comparable or larger than the magnetic energy density. An increase in thermal emission and energy density from the photosphere would lead to an increase in the Compton cooling and emission from the non-thermal electrons. This would naturally explain the close correlation between the components and that they occur approximately simultaneously. The variation in  $s$  from  $\sim -1.5$  to  $\sim -2$  would then be interpreted as  $\nu_{\min}$  approaching  $kT$ .

The temperature is shown above to decay as  $T \propto t^{-\kappa} \propto R^{-\kappa}$  during the coasting phase. The thermal energy flux goes as  $F_{\text{BB}} \propto AT^4$ , where  $A$  is the emitting surface. Due to relativistic aberration of light, the surface visible to an observer at infinity is  $A = \pi R^2/\Gamma^2$ . Therefore,  $F_{\text{BB}} \propto T^{4-2/\kappa}$  and typical values of  $\kappa = [0.67, 1.5]$  give  $F_{\text{BB}} \propto T^\eta$  with  $\eta = [1.0, 2.7]$ . It was further noted above that the total measured flux is approximately proportional to the thermal flux component, since the two components track each other. Therefore, the last relation reproduces the power-law hardness-intensity correlation, which pulses commonly exhibit, and the distribution of its power-law indices which was determined to be  $1.9 \pm 0.7$  by Borgonovo & Ryde (2001).

I wish to thank Drs. C. Björnsson, C. Fransson, P. Mészáros, and M. Rees for useful discussions. I also thank the referee for constructive criticism and Karin Ryde for assistance with the language. Support for this work was given by the Swedish Research Council.

## REFERENCES

- Amati et al. 2002, A&A, 390, 81  
 Band, D., et al. 1993, ApJ, 413, 281  
 Baring, M.G., & Braby, M.L. 2004, ApJ, 613, 460

- Borgonovo, L. & Ryde, F. 2001, ApJ, 548, 770
- Bussard, R.W., ApJ, 284, 357
- Crider, A., et al. 1997, ApJ, 479, L39
- Daigne, F. & Mochkovitch, R. 2002, MNRAS, 336, 1271
- Drenkhahn, G., & Spruit, H. C. 2002, A&A, 391, 1141
- Fishman, G.J., & Meegan, C.A. 1995, ARAA, 33, 415.
- Ghirlanda, G., Celotti, A., & Ghisellini, G. 2003, A&A, 406, 879
- Ghirlanda, G., Ghisellini, G., & Lazzati, D. 2004, ApJ, 616, 331
- Ghisellini, G., Celotti, A., Lazzati, D. 2000, MNRAS 313, L1
- Ghisellini, G., Lazzati, D., Celotti, A., & Rees, M. J. 2000, MNRAS, 316, L45
- Grimsrud, O. M., & Wasserman, I. 1998, MNRAS, 300, 1158
- Katz, J. I. 1994, ApJ, 432, L107
- Kaneko, Y., Preece, R. D., & Briggs, M. S. 2003, AAS, 203, 8004
- Kocevski, D., Ryde F., & Liang E., 2003, ApJ, 596, 389
- Kobayashi, S., Ryde, F., & MacFadyen, A. 2002, ApJ, 577, 302
- Lloyd-Ronning, N. M., Petrosian, V., & Mallozzi, R. S. 2000, ApJ, 534, 227
- Lloyd-Ronning, N. & Petrosian, V. 2000, ApJ, 543, 722
- Lyutikov, M. & Usov, V. V. 2000, ApJ, 543, L129
- Mészáros, P. 2002, ARA&A, 40, 137
- Mészáros, P., Laguna, P., & Rees, M. J. 1993, ApJ, 415, 181
- Mészáros, P., & Rees, M. J. 2000, ApJ, 530, 292
- Pacholczyk, A. G. 1970, *Radio Astrophysics* (San Francisco: W. H. Freeman and Co.)
- Pe'er, A., & Waxman, E. 2004, ApJ, 613, 448

Preece, R. D., Briggs, M. S., Mallozzi, R. S., Pendleton, G. N., Paciesas, W. S., & Band, D. L. 2000, *ApJSS*, 126, 19

Ramirez-Ruiz, E., & Lloyd-Ronning, N.M. 2002, *NewA*, 7, 197

Rees, M. J., & Mészáros, P. 2005, submitted

Ryde, F. 2004, *ApJ*, 614, 827

Stern, B. & Poutanen, J. 2004, *MNRAS*, in press

Tavani, M. 1996, *ApJ*, 466, 768

Zhang, B. & Mészáros, P. 2002, *ApJ*, 581, 1236



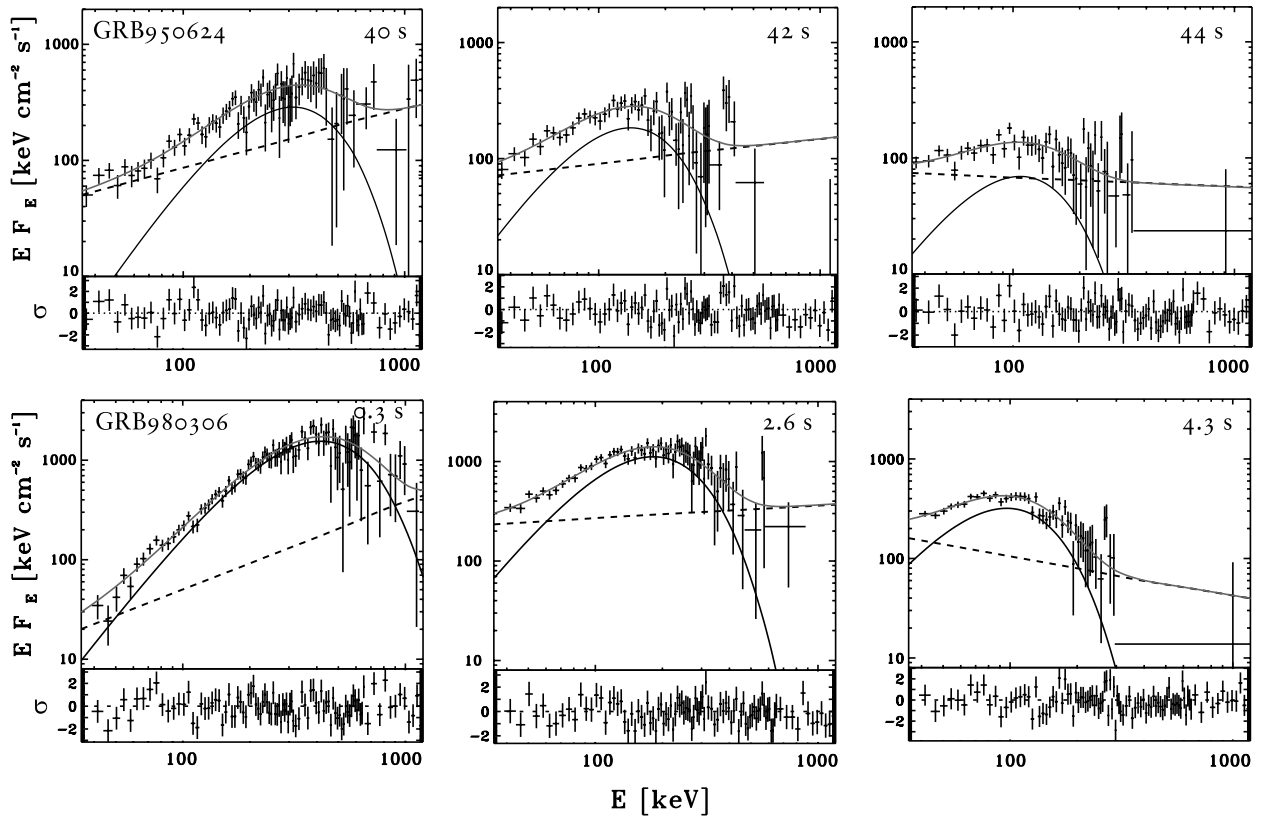


Fig. 1.— Hybrid-model spectral-fits to *CGRO* BATSE data ( $\sim 20 - 1900$  keV) for two bursts discussed in the text (GRB950624, GRB980306). The time after the trigger of the fitted bin is given in the upper right-hand corner. Note that the investigated pulse in GRB950624 started at 39.8 s. The non-thermal component is represented by the dashed line, the thermal component by the thick line, and the summed spectrum by the grey line. The spectral data points are rebinned to achieve a signal-to-noise ratio of unity.

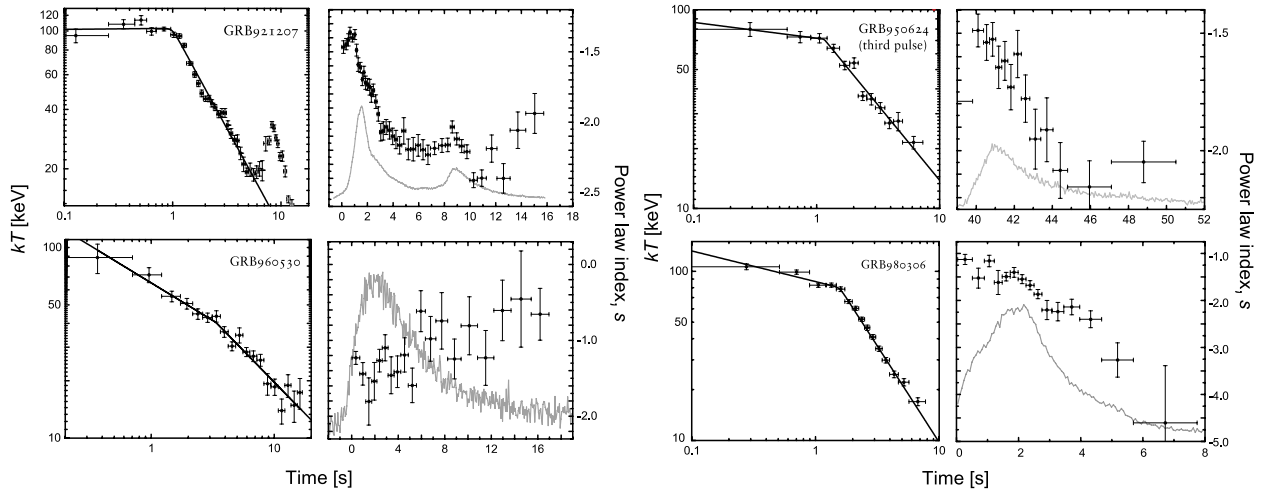


Fig. 2.— Evolution of  $kT$  (left) and power-law index,  $s$  (right). The grey curves are the detector count light-curves, with arbitrary normalization. The time is counted from the trigger, except for in the plot of  $kT$  of GRB950624, where time is from the beginning of that pulse.

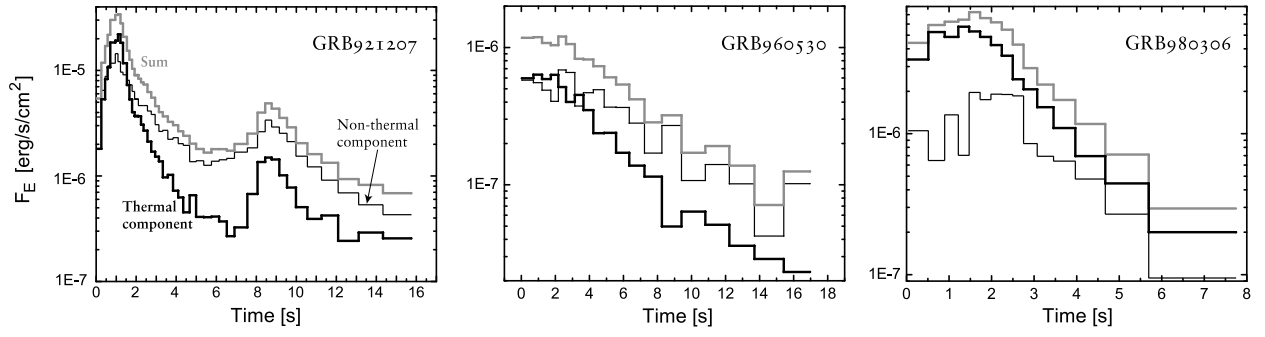


Fig. 3.— Energy-flux light-curves of the two separate components; thermal (bold line), and non-thermal (thin line). The total light-curves are depicted by the grey lines. After the break-time the thermal light-curves are approximate power-laws (note the linear time-axis).